Distributed MIMO network for 5G enhanced mobile broadband

Fumiyuki Adachi, Amnart Boonkajay, Tomoyuki Saito, Yuta Seki

Fumiyuki Adachi, Amnart Boonkajay, Tomoyuki Saito, Yuta Seki, "Distributed MIMO network for 5G enhanced mobile broadband," Proc. SPIE 10559, Broadband Access Communication Technologies XII, 1055909 (29 January 2018); doi: 10.1117/12.2291321

Event: SPIE OPTO, 2018, San Francisco, California, United States

Distributed MIMO Network for 5G Enhanced Mobile Broadband

Fumiyuki Adachi, Amnart Boonkajay, Tomoyuki Saito, Yuta Seki
Research Organization of Electrical Communication, Tohoku University
2-1-1 Katahira, Aoba-ku, Sendai, 980-8577 Japan

ABSTRACT

One of important applications in 5G mobile communications is the enhanced mobile broadband (eMBB). A promising approach for achieving 5G eMBB under the limited radio bandwidth and energy is an introduction of a small-cell structured network. An advanced utilization of multi-input multi-output (MIMO) transmission is also another possible approach. First, the conceptual structure of distributed MIMO network is introduced. A number of distributed antennas (DAs) are deployed over a macro-cell area and they are connected to a macro-cell base station (MBS) via optical mobile fronthaul. Then, we present the recent advances in distributed MIMO cooperative transmission, i.e., space-time block coded transmit diversity (STBC-TD) for improving the link capacity of a macro-cell edge area, minimum mean square error multiuser multiplexing combined with singular value decomposition (MMSE-SVD) for increasing the sum capacity, and blind selective mapping (SLM) for reducing the transmit signal peak-to-average power ratio (PAPR).

Keywords: 5G, distributed MIMO, optical mobile fronthaul, cooperative transmission, space-time block coded transmit diversity, MMSE multiplexing, singular value decomposition, selected mapping

1. INTRODUCTION

The 1st generation (1G) mobile communications network services started in December 1979 in Japan. Since then, we witnessed the new generation approximately every 10 years as seen from Fig. 1. The mobile communications networks have evolved into the 4th generation (4G) in 2015. Now, almost everyone is connected to the networks and the mobile communications networks have become an important infrastructure of our modern society. The major communication service was voice conversation over the mobile phone. After the introduction of digital 2G, the major communications services have shifted from the voice to data. More and more mobile users started to access the Internet. Since the start of 3G services, video communications have been getting increasingly popular. The mobile data traffic volume in 2020 will reach about 1,000 times of 2010. Now 3.9G called long-term evolution (LTE) [1] and 4G called LTE-Advanced (LTE-A) are being rapidly deployed worldwide. LTE-A services started in March 2015 in Japan [2]. Video communications and data services will become more popular. In 5G, broadband data services of peak data rate of >10Gbps, known as enhanced mobile broadband (eMBB), are expected. Recently, the development of 5G network is on-going worldwide aiming at the introduction of 5G in around 2020 [3].

In analog 1G, the coverage expansion was the most important technical issue. However, the important technical issue after digital 2G is to achieve as higher speed data transmission as possible under the limited available bandwidth and power (or energy) while suppressing the inter-cell interference (ICI) to a certain degree. Maximizing the area spectrum efficiency (ASE) in bps/Hz/km^2 and the energy efficiency (EE) in bits/Joule is required. A key for realizing 5G networks is an advanced utilization of spatial domain (massive MIMO and distributed antennas). The antenna will become one of radio resource in addition to frequency, time, and power. In addition to enrich the broadband data services, 5G will provide new other communications services, e.g., massive machine type communications (mMTC) and ultra-reliable and low latency communications (uRLLC) [4], as seen from Fig. 2. In 5G, the radio resource management which efficiently assigns the communication time and bandwidth among a huge number of mobile communications devices will become another important technical issue toward 5G as seen in Fig. 3.

A possible approach for improving the ASE and the EE simultaneously is to adopt a small-cell structured network. Reducing the base station (BS) coverage area (i.e., small-cell) enables the same frequency to be reused more densely in the same service area and accordingly, the ASE can be improved. The short range communication lowers the transmit signal power significantly, thereby the EE can be improved. However, frequent handover may happen, thereby leading to

Broadband Access Communication Technologies XII, edited by Benjamin B. Dingel,
Katsutoshi Tsukamoto, Spiros Mikroulis, Proc. of SPIE Vol. 10559, 1055909

the increased control signal traffic which reduce the capacity of data traffic. Besides straightforwardly reducing the cell size, the large-scale multi-input multi-output (MIMO) can be applied in order to avoid frequent handover.

In this paper, we firstly introduce the conceptual structure of distributed MIMO network, which consists of macro BS (MBS), a number of distributed antennas (DAs) deployed over a macro-cell area, and optical mobile fronthaul connecting MBS and DAs. Then, we present the recent advances in distributed MIMO cooperative transmission, i.e., space-time block coded transmit diversity (STBC-TD) for improving the link capacity of a macro-cell edge area, minimum mean square error multiuser multiplexing combined with singular value decomposition (MMSE-SVD) for increasing the sum capacity, and blind selected mapping (SLM) for reducing the transmit signal peak-to-average power ratio (PAPR). The PAPR reduction is important, in particular, when higher frequency band, e.g., mm-wave band, is utilized [5].

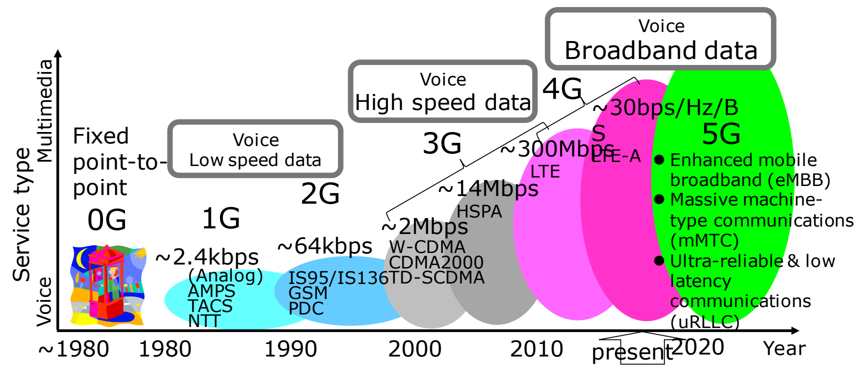

Fig. 1 Mobile communications evolution.

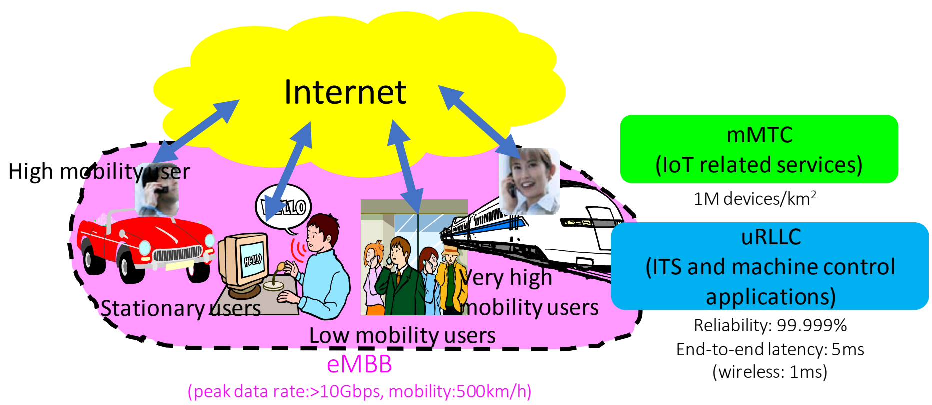

Fig. 2 5G communications services.

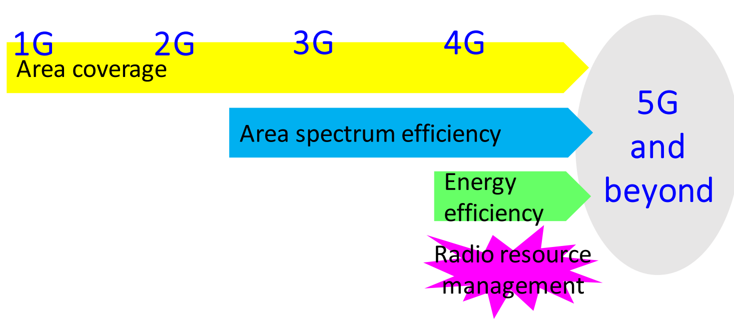

Fig.3 Technical issues toward 5G.

2. CONCEPTUAL STRUCTURE OF DISTRIBUTED MIMO NETWORK

2.1 Co-located MIMO versus distributed MIMO

The large-scale MIMO can effectively form a large number of user-centric small cells. It can be classified into co-located (or massive) MIMO and distributed MIMO. Co-located MIMO and distributed MIMO are compared in Fig.4. The former approach is to use a large number of co-located antennas at the MBS [6] while the latter approach is to spatially deploy a large number of DAs over a macro-cell area [7-10]. In distributed MIMO, short-range link reduces the transmit power while, in co-located MIMO, a significant antenna-gain increase can offset the propagation path loss [11]. Therefore, to solve the limited bandwidth problem, it is possible to utilize new frequency bands like mm-wave band, where abundant bandwidth remains unused. The handover is replaced with beam selection in the co-located MIMO while it is replaced with antenna selection in the distributed MIMO. If the user equipment (UE) moves from one MBS area into another, then the handover process is initiated. The handover rate remains similar to that experienced in 4G. In co-located MIMO, a number of narrow beams are formed, each illuminates a different UE. However, the beam width may become wider due to local scatters surrounding UE of interest and accordingly, may interfere to each other. Furthermore, some beams may be blocked by buildings located between a MBS and a UE. On the other hand, in distributed MIMO, some DAs can be selected by taking into account blockage or shadowing. A possible advantage of using distributed MIMO over co-located MIMO is its capability of alleviating problems arising from the blockage or shadowing.

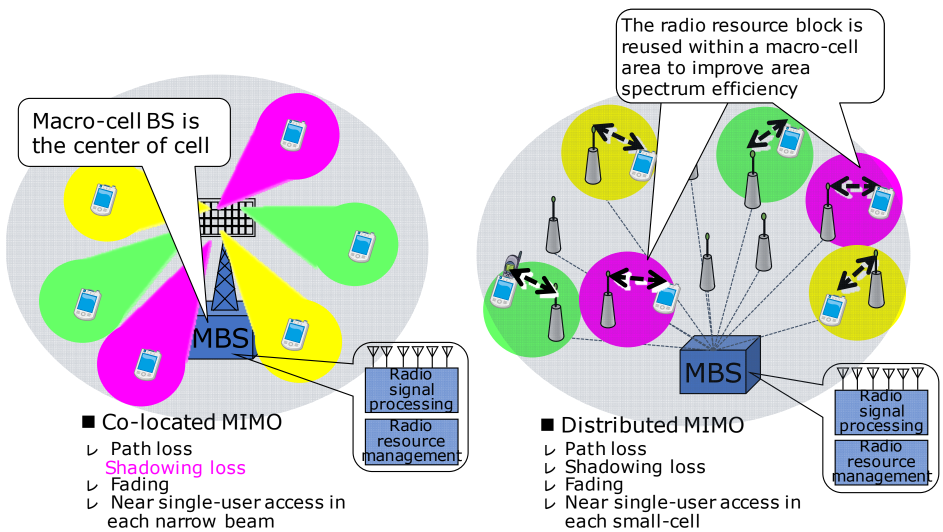

Fig. 4 Co-located MIMO versus distributed MIMO.

2.2 Conceptual structure of distributed MIMO

The conceptual structure of distributed MIMO is illustrated in Fig. 5. All DAs are connected to MBS by optical mobile fronthaul. Each MBS performs the radio signal processing for signal transmission and reception using cooperative transmission technique [12]. A predetermined number of distributed antennas near a UE are selected to form a user-centric small-cell. For a high mobility UE, the MIMO channel between UE antennas and selected DAs may change during the signal transmission. However, as far as the propagation time difference among DAs are within the cyclic prefix (CP) length for block transmissions using OFDM and SC with frequency-domain equalization (FDE), this problem can be replaced with channel estimation problem.

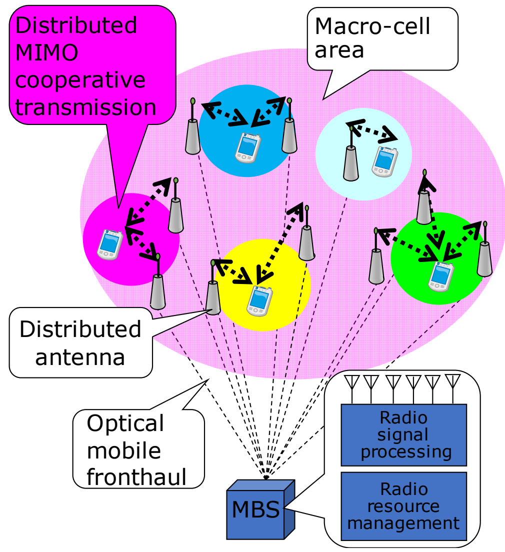

Fig. 5. Conceptual structure of distributed MIMO.

2.3 Optical mobile fronthaul

The optical mobile fronthaul plays an important role in 5G. The radio over fiber (RoF) technology applicable for optical mobile fronthaul is summarized in Table 1. Since the nonlinearity of analog RoF link causes a serious problem, digital RoF is adopted, which transmits digitized baseband I/Q signals using the common public radio interface (CPRI) [13]. Using CPRI, the distributed antenna side needs simple RF modulator and amplifier only, but the optical bandwidth becomes 16 times wider than the radio signal bandwidth if simple optical intensity modulation (IM) is applied. The peak data rate of 5G will become >10 Gbps and hence, a significant bandwidth reduction is indispensable. Instead of using binary IM, higher-level digital coherent modulation should be employed [14, 15]. However, even if 1024 quadrature amplitude modulation (QAM) is used, the bandwidth expansion ratio is still 1.6.

Optical and radio signals are both of an electromagnetic signal type and the difference between two is only the carrier frequency. An introduction of fully coherent RoF to optical mobile fronthaul may be effective in both reducing the bandwidth and latency. Fully coherent RoF treats the optical transmission and radio transmission similarly by removing analog-digital converter (ADC) and digital-analog converter (DAC) [16-18] as shown in Fig. 6. This is the real radio-optical convergence. For implementing the distributed MIMO cooperative transmission, optical mobile fronthaul should have a low latency property. The wavelength division multiplexing (WDM) may be much promising instead of time division multiplexing (TDM). Combining fully coherent RoF and WDM can realizes the bandwidth efficient and low latency optical mobile fronthaul. Since the concatenation of RoF link and radio link can be treated as an equivalent radio link, all of radio signal processing including modulation/demodulation, equalization, etc, can be done at MBS.

Table 1. RoF technology for mobile fronthaul.

RoF type	Waveform type	Remarks
Analog RoF	Real-valued analog RF waveform	☐ Intensity modulation ☐ Nonlinear optical distortion
Digital RoF ■ Noncoherent ■ Coherent	Digitized real-valued I and Q waveforms	☐ A/D, D/A of I and Q waveforms ☐ Noncoherent/coherent modulation ☐ Bandwidth expansion (x16/$\log_2 M$)
Fully coherent RoF	Complex-valued analog I+jQ waveform	☐ Removal of A/D and D/A converters and direct up/down conversion between optical and radio frequencies ☐ Equalization in baseband

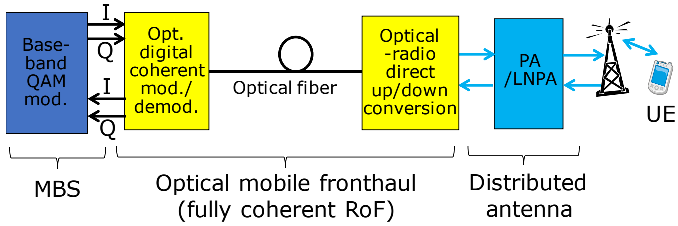

Fig. 6 Fully coherent RoF.

3. DISTRIBUTED MIMO COOPERATIVE TRANSMISSION

The signal bandwidth in 5G will be wider than 100MHz. The radio channel experiences a strong frequency-selectivity and therefore, some powerful equalization technique such as frequency-domain equalization (FDE) needs to be jointly used with cooperative transmission. The use of time division duplex (TDD) allows equalization processing for both uplink (UE→MBS) and downlink (MBS→UE) transmissions at an MBS as shown in Fig. 7. This greatly simplifies the radio signal processing at UE. A simplified transmitter/receiver structure of distributed MIMO cooperative uplink transmission is illustrated in Fig. 8. Similar to LTE-Advanced, we assume OFDM for downlink transmission and SC for uplink transmission.

For improving the link capacity of a macro-cell edge UE, space-time coded transmit diversity (STBC-TD) is applied. The simple Alamouti code [19] is used. By combining maximal ratio transmit diversity (MRT)-FDE and MMSE-FDE with STBC-TD for downlink transmission an uplink reception, respectively, an arbitrary number of distributed antennas can be used to obtain a large diversity gain [20] although the number of UE antennas is limited to 6. For increasing the sum capacity, MMSE-SVD is applied. The inter-user interference (IUI) is suppressed by multi-user MMSE-FDE assuming eigenmode downlink reception/uplink transmission at UE. The inter-antenna interference (IAI) is suppressed by eigenmode reception/transmission using singular value decomposition (SVD) [21]. Multi-user MMSE-SVD provides lower outage probability than single-user STBC-TD in a high link capacity region. However, in a low link capacity region (i.e., UEs near the macro-cell edge), the outage probability is higher with multi-user MMSE-SVD than with single-user STBC-TD.

When the cooperative transmission is used, the transmit signal PAPR increases. Some PAPR reduction technique is necessary if high SHF or mm-wave band is used. To reduce the transmit signal PAPR, blind SLM is applied. SLM multiplies an appropriate phase rotation sequence to the transmit signal in the frequency-domain or in the time-domain to minimize the PAPR [22]. Both the transmitting and receiving sides share the same sequence book. The conventional SLM informs the side information (phase-rotation sequence index) to the receiving side to recover the original signal. Since the side information transmission needs to be error-free, it is typically coded with low-rate forward error correction (FEC), consequently reduces the spectrum efficiency. The received signal constellation is significantly distorted if the receiving side applies an incorrect phase rotation sequence. Blind SLM exploits this fact and estimates the phase rotation sequence based on MMSE criterion without the help of side information.

For distributed MIMO cooperative transmission, multiple DAs near a UE must be selected first and then, the channel state information (CSI) of MIMO channel between selected DAs and UE antennas must be estimated. The subframe structure supporting the selection of DAs and the MIMO channel estimation is illustrated in Fig. 9. The subframe consists of the uplink pilot time slot (UpPTS) and the downlink pilot time slot (DwPTS) followed by 12 data time slots (DTSs). The transmission efficiency is kept the same as 3GPP Rel.10 subframe structure [23]. Each TS length is equal to one OFDM symbol plus cyclic prefix (CP) length. First, the scheduled UE transmits the orthogonal frequency-multiplexed uplink pilot from UE antennas. MBS performs the channel estimation to select multiple DAs. Then, MBS transmits the orthogonal frequency-multiplexed downlink pilot from the selected DAs for MIMO channel estimation at UE. In this way, exploiting the channel reciprocity because of TDD, the CSI of MIMO channel can be shared by MBS and UEs without feedback [24].

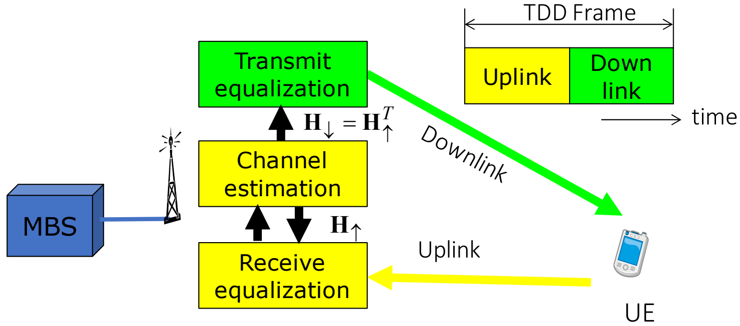

Fig. 7 TDD allows both uplink and downlink equalization at an MBS.

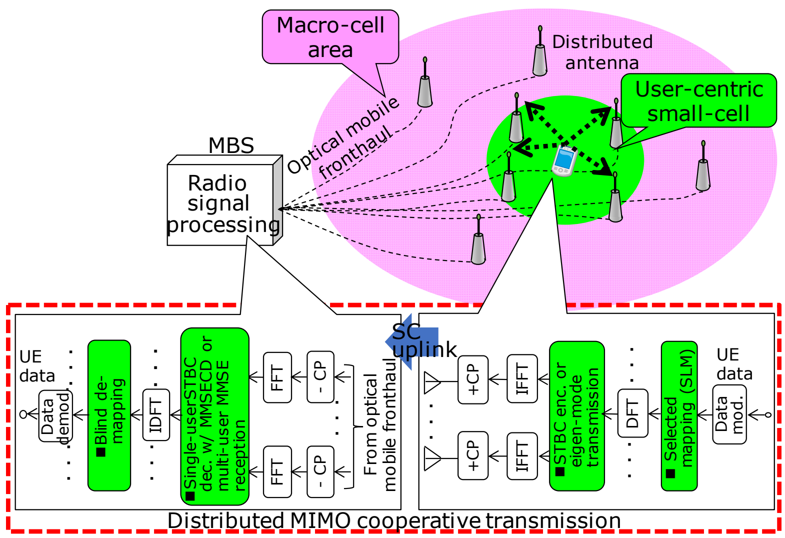

Fig. 8. MIMO cooperative transmitter/receiver structure for SC uplink.

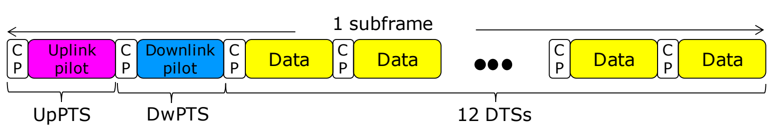

Fig. 9 Subframe structure.

4. COMPUTER SIMULATION

The uplink link capacity was examined by computer simulation. It is assumed that the MBS area of interest is surrounded by 6 adjacent MBS areas. 19 DAs are deployed regularly or randomly in each MBS area, while 2 UEs, each equipped with 2 antennas, are randomly located. 4 DAs are selected for distributed MIMO cooperative transmission. The system band consisting of 1024 subcarriers is considered. Assuming the subcarrier separation of 75 kHz and the CP of 1.67μs (equivalent to a maximum path length difference of 500m), the system bandwidth and the subframe length become 76.8MHz and 0.209ms, respectively. A frequency-selective fading channel having 16-path uniform power delay profile (PDP) is assumed as well as a log-normally distributed shadowing loss with standard deviation of 7 dB and a path loss with path loss exponent of 3.5. The channel is assumed to be a quasi-static Nakagami-Rice fading channel with K factor of 10dB when the distance between DA and UE is shorter than $1/19^{1/2}$ times the radius of the macro-cell area, otherwise quasi-static Rayleigh fading is assumed.

The spatial and cumulative distributions of the uplink throughput obtained by computer simulation are illustrated in Fig. 10 and Fig. 11, respectively. It can be clearly seen that the distributed MIMO provides high throughput over nearly entire MBS area, while the co-located MIMO provides high throughput only near the MBS. It is also seen that the single-user STBC-TD can provide higher throughput than multi-user MMSE-SVD near the macro-cell edge, where the uplink signal received at MBS is weak and is thus strongly affected by the ICI from UEs in surrounding MBS areas.

Figure 12 plots how blind SLM reduces the PAPR of SC uplink signal when the number of subcarriers is 128. It can be obviously seen from Fig. 12 that PAPR reduces when the number of phase rotation sequences increases. Figure 13 plots the achievable uncoded BER performances of SC uplink using STBC-TD and MMSE-SVD in a quasi-static Rayleigh fading and assuming the subframe structure shown in Fig. 9 (note that the transmit and receive FDE weights are generated based on the CSI obtained from UpPTS and DwPTS, respectively). The propagation path-loss and shadowing-loss are neglected for simplicity. Without blind SLM, it is seen from Fig. 13(a) that both STBC-TD and MMSE-SVD achieve the same BER as those with ideal CSI. STBC-TD achieves better BER than MMSE-SVD because of larger diversity gain. In Fig. 13(b), the blind SLM achieves the BER performance almost identical to the case of transmission without blind SLM.

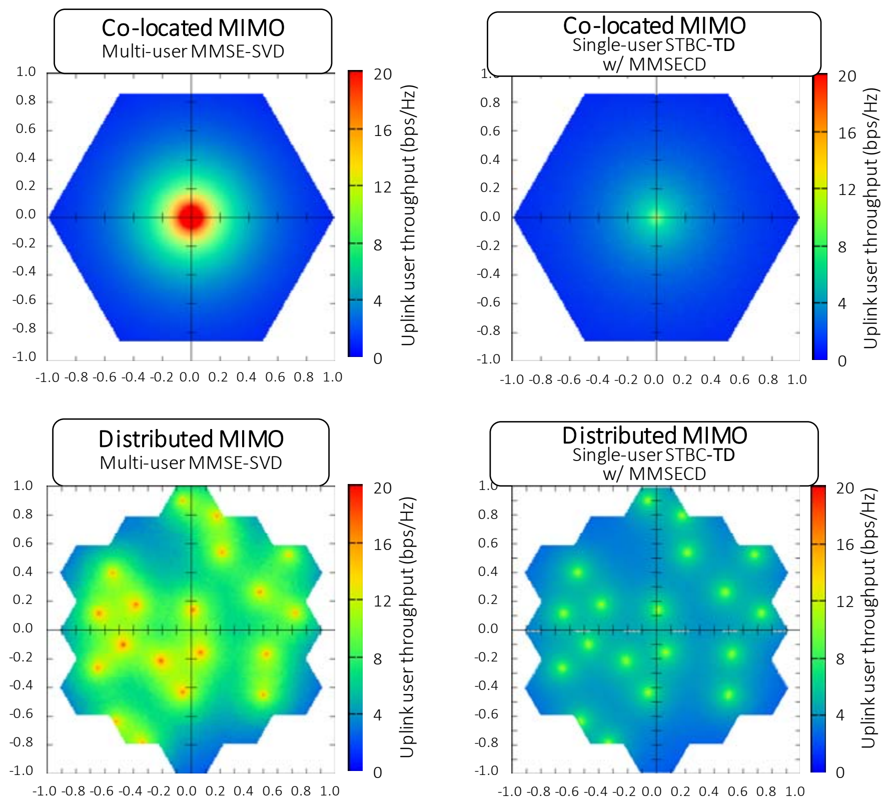

Fig. 10 Spatial distribution of uplink user throughput over an MBS area.

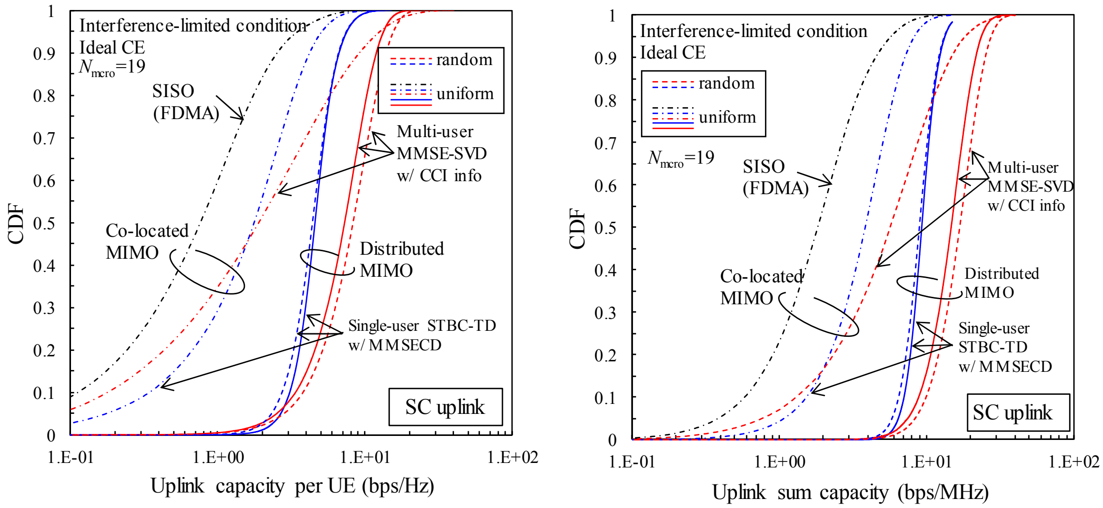

Fig. 11 Uplink throughput performance.

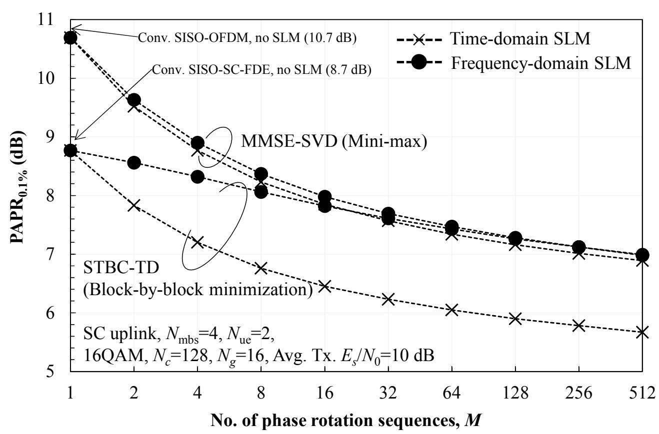

Fig. 12 PAPR reduction by blind SLM.

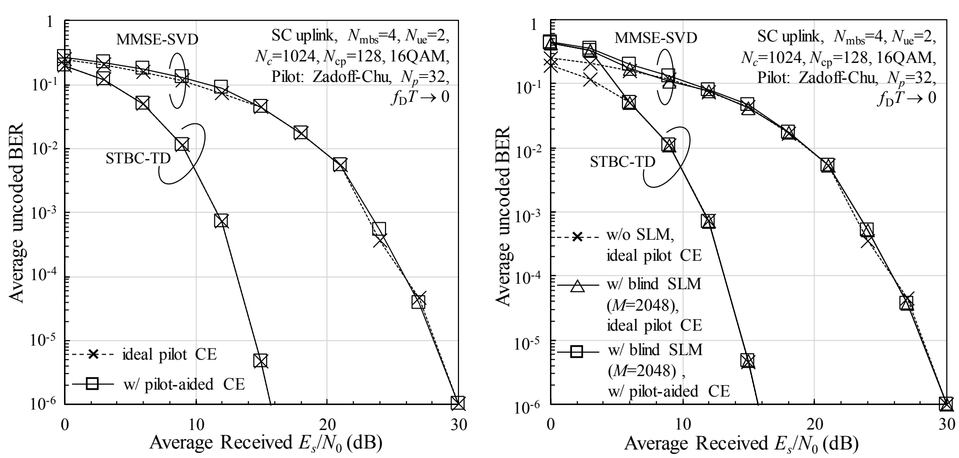

(a) Without blind SLM (b) With blind SLM

Fig. 13 BER performances of SC uplink using STBC-TD and MMSE-SVD.

5. CONCLUSION

In this paper, after overviewing the wireless evolution of mobile communications technology over the past 35 years, we discussed about the technical issues toward 5G. Then, the recent advances in distributed MIMO was presented. Higher deployment cost is expected in distributed MIMO since spatially deployed distributed antennas need to be connected by optical mobile fronthaul. A hybrid MIMO (between co-located MIMO and distributed MIMO) may be a practical solution to balance the transmission performance and system deployment cost.

Acknowledgement: The results presented in this paper have been achieved by "The research and development project for realization of the fifth-generation mobile communications system," commissioned to Tohoku University by The Ministry of Internal Affairs and Communications (MIC), Japan.

REFERENCES

[1] D. Astély, et al., "LTE: The evolution of mobile broadband," IEEE Commun. Mag., Vol. 47, No. 4, pp. 44-51, April, 2009.
[2] NTTDOCOMO Tech. J, Vol.23, No.2, July, 2015.
[3] C. X. Wang, et al., "Cellular architecture and key technologies for 5G wireless communication networks," IEEE Commun. Mag., Vol. 52, Issue 2, pp. 122-130, Feb., 2014.
[4] ITU-R Recommendations M2083-0: IMT Vision – Framework and overall objectives of the future development of IMT for 2020 and beyond, Sept. 2015.
[5] W. L. Chan and J. R. Long, "A 58-65 GHz Neutralized CMOS Power Amplifier with PAE above 10% at 1-V Supply," IEEE Journal of Solid-State Circuits, Vol. 45, No. 3, pp. 554-564, Mar. 2010.
[6] DOCOMO 5G White Paper, 5G radio access: requirements, concept and technologies, July, 2014 (https://www.nttdocomo.co.jp/english/corporate/technology/whitepaper_5g/).
[7] F. Adachi, K. Takeda, T. Obara, T. Yamamoto, and H. Matsuda, "Recent advances in single-carrier frequency-domain equalization and distributed antenna network," IEICE Trans. Fundamentals, Vol. E93-A, No. 11, pp. 2201-2211, Nov., 2010.
[8] F. Adachi, W. Peng, T. Obara, T. Yamamoto, R. Matsukawa, and M. Nakada, "Distributed antenna network for gigabit wireless access," Int. J. of Electronics and Commun. (AEUE), Elsevier, Vol. 66, Issue 6, pp. 605-612, 2012. doi: 10.1016/j.aeue.2012.03.010.
[9] A. A. M. Saleh, A. J. Rustako, and R. S. Roman, "Distributed antennas for indoor radio communications," IEEE Trans. Commun., Vol. 35, No.12, pp. 1245-1251, Dec., 1987.
[10] W. Choi and J.G. Andrews, "Downlink performance and capacity of distributed antenna systems in a multicell environment," IEEE Trans. Wireless Commun., Vol. 6, No. 1, pp. 69-73, Jan., 2007.
[11] T. L. Marzetta, "Noncooperative cellular wireless with unlimited numbers of BS antennas," IEEE Trans. Wireless Commun., Vol. 9, No. 11, pp. 3590-3600, Nov. 2010.
[12] F. Adachi, A. Boonkajay, Y. Seki, T. Saito, S. Kumagai, and H. Miyazaki, "Cooperative Distributed Antenna Transmission for 5G Mobile Communications Network," IEICE Trans. Commun., Vol.E100-B, No.8, pp. 1190-1204, Aug., 2017. http://doi.org/10.1587/transcom.2016FGP0019.
[13] http://www.cpri.info/index.html.
[14] K. Kikuchi, "Digital coherent optical communication systems: fundamentals and future prospects," IEICE Electronics Express, Vol. 8, No.20, pp.1642-1662, Oct. 2011. doi:10.1587/elex.8.1642.
[15] T. Omiya, M. Yoshida, and M. Nakazawa, "400 Gbit/s 256 QAM-OFDM transmission over 720 km with a 14 bit/s/Hz spectral efficiency by using high-resolution FDE," Opt. Express, Vol. 21, No. 3, pp. 2632-2641, Feb., 2013.
[16] F. Adachi, "Radio and optical convergence in 5G," OFC Workshop: How will Optical Technologies Support Wireless Communications in 5G and beyond?, Anaheim Convention Center, Anaheim, California, USA, 20-24 March, 2016.
[17] F. Adachi, "Wireless network evolution toward 5G network," Proc. 21st Optoelectronics and Communications Conference /International Conference on Photonics in Switching 2016 (OECC/PS2016), Niigata, Japan, 3-7 July, 2016.

[18] F. Adachi, "Wireless evolution toward 5G mobile communications network," The 24th Congress of the International Commission for Optics (ICO-24), Shinjuku, Japan, 21-25 Aug., 2017.
[19] S. M. Alamouti, "A simple transmit diversity technique for wireless communications," IEEE J. Sel. Areas Commun., Vol. 16, No. 8, pp. 1451–1458, Oct., 1998.
[20] R. Matsukawa, T. Obara, and F. Adachi, "Frequency-domain space-time block coded single-carrier distributed antenna network," IEICE Communications Express (ComEX), Vol. 2, No. 4, pp. 141-147, 15 April, 2013.
[21] S. Kumagai and F. Adachi, "Joint Tx/Rx MMSE filtering for single-carrier MU-MIMO uplink," Proc. 2015 IEEE 12nd Vehicular Technology Society Asia Pacific Wireless Communications Symposium (APWCS 2015), Singapore, 19-21 Aug., 2015.
[22] A. Boonkajay and F. Adachi, "A blind selected mapping technique for low-PAPR single-carrier signal transmission," Proc. Int. Conf. Info. Commun.and Signal Proc. (ICICS 2015), Singapore, 2-4 Dec., 2015.
[23] E. Dahlman, S. Parkvall and J. Skold, 4G: LTE-Advanced Pro and the Road to 5G, 3rd-ed., Elsevier, 2016.
[24] F. Adachi, A. Boonkajay, T. Saito, and Y. Seki, "A study on channel estimation for time-division duplex distributed antenna cooperative transmission," IEICE Technical Report, Vol.116, No.394, RCS2016-263, pp.159-164, Jan., 2017.